

Biomechanical Mapping of the Female Pelvic Floor: Uterine Prolapse Versus Normal Conditions

Vladimir Egorov^{1*}, Vincent Lucente², S Abbas Shobeiri³, Peter Takacs⁴, Lennox Hoyte⁵ and Heather van Raalte⁶

¹Artann Laboratories, Trenton, United States

²The Institute for Female Pelvic Medicine and Reconstructive Surgery, Allentown, United States

³NOVA Fairfax Hospital, Falls Church, United States

⁴Eastern Virginia Medical School, Norfolk, United States

⁵The Pelvic Floor Institute, Tampa, United States

⁶Princeton Urogynecology, Princeton, United States

*Corresponding Author: Vladimir Egorov, Artann Laboratories, Trenton, United States

Received: August 09, 2018 ; Published: October 31, 2018

Abstract

Introduction: Quantitative biomechanical characterization of pelvic supportive structures and functions in vivo is thought to provide insight into the pathophysiology of pelvic organ prolapse (POP). Vaginal tactile imaging is an innovative approach to the biomechanical mapping of the female pelvic floor to quantify tissue elasticity, pelvic support, and pelvic muscle functions. The Vaginal Tactile Imager (VTI) records high definition pressure patterns through the vaginal walls under an applied tissue deformation and during pelvic floor muscle contractions.

Objective: The objective of this study is to explore an extended set of 52 biomechanical parameters of the female pelvis for the differentiation and characterization of uterine prolapse relative to normal pelvic floor conditions.

Methods: Sixty subjects were included in the data analysis from observational and case-controlled studies. Out of these 60, forty-two subjects had normal pelvic floor conditions and 18 subjects had uterine prolapse (no anterior, no posterior prolapse). The VTI, model 2S, was used with an analytical software package to automatically calculate 52 biomechanical parameters for 8 VTI test procedures (probe insertion, elevation, rotation, Valsalva maneuver, voluntary muscle contractions in 2 planes, relaxation, and reflex contraction).

Results: The ranges, mean values, and standard deviations for all 52 VTI parameters were established. Twenty-two of 52 parameters were identified as statistically sensitive ($p < 0.05$; t-test) to the development of uterine prolapse. Among these 21 parameters, 6 parameters show changes (decrease) in tissue elasticity, 5 parameters show deteriorations in pelvic support, and 10 parameters show weakness in muscle functions for uterine prolapsed versus normal conditions.

Conclusion: The biomechanical mapping of the female pelvic floor with the VTI provides a unique set of parameters characterizing uterine prolapse versus normal conditions. These objectively measurable biomechanical transformations of pelvic tissues, support structures, and functions under the prolapse conditions may be useful in future research and practical applications.

Keywords: Biomechanical Mapping; Female Pelvic Floor; Uterine Prolapse; Tissue Elasticity; Pelvic Support; Pelvic Function; Tactile Imaging

Introduction

A recent survey identified the highest priority research questions pertaining to the pathophysiology and treatments of pelvic organ prolapse (POP). According to the survey, mechanistic research on pelvic supportive structures, clinical trials to optimize outcomes after POP surgery and evidence-based quality measures for POP outcomes are among the major focus areas [1]. In vaginal prolapse surgery, about 20% of procedures are performed for recurrent POP. There are not many other reconstructive surgical fields with such poor surgical outcomes [2].

Many pelvic floor disorders, including POP, stress urinary incontinence (SUI), sexual dysfunction, congenital anomalies, and others, are clearly manifested in the mechanical properties of pelvic organs. Therefore, biomechanical mapping of a tissue response to applied pres-

sure or load within the pelvic floor opens new possibilities in biomechanical assessment and monitoring of pelvic floor conditions. The newly developed vaginal tactile imaging allows biomechanical mapping of the female pelvic floor including assessment of tissue elasticity, pelvic support, and pelvic muscle functions in high definition [3-6].

Previously, we reported the intra- and inter-observer reproducibility of vaginal tactile imaging [7] and proposed interpretation of biomechanical mapping of the female pelvic floor [8]. The new mechanistic parameters were introduced for assessment of the vaginal [9] and pelvic floor conditions [10].

Objective of the Study

The objective of this study is to identify an extended set of Vaginal Tactile Imager (VTI) parameters which would comprehensively characterize the pelvic floor tissues including supportive structures and their biomechanical functions contributing to the development of uterine prolapse (UP).

Material and Methods

Definitions

Tactile Imaging is a medical imaging modality translating the sense of touch into a digital image [10]. The tactile image is a function of $P(x, y, z)$, where P is the pressure on soft tissue surface under applied deformation and x, y and z are the coordinates where P was measured. The tactile image is a "pressure map" on which the direction of tissue deformation must be specified.

Functional Tactile Imaging translates muscle activity into dynamic pressure pattern $P(x, y, t)$ for an area of interest, where t is time and x and y are coordinates where pressure P was measured. It may include: (a) muscle voluntary contraction, (b) involuntary reflex contraction, (c) involuntary relaxation, and (d) specific maneuvers.

Biomechanical Mapping = Tactile Imaging + Functional Tactile Imaging

A tactile imaging probe has a pressure sensor array mounted on its face that acts similar to human fingers during a clinical examination, deforming the soft tissue and detecting the resulting changes in the pressure pattern on the surface. The sensor head is moved over the surface of the tissue to be studied, and the pressure response is evaluated at multiple locations along the tissue. The results are used to generate 2D/3D images showing pressure distribution over the entire area of the tissue under study.

Generally, an inverse problem solution for tactile image $P(x, y, z)$ would allow the reconstruction of tissue elasticity distribution (E) as a function of the same coordinates $E(x, y, z)$. Unfortunately, the inverse problem solution is hardly possible for most real objects because it is a non-linear and ill-posed problem. However, the tactile image $P(x, y, z)$ per se reveals tissue or organ anatomy and elasticity distribution because it maintains the stress-strain relationship for deformed tissue [11,12]. Thus the spatial gradients $\partial P(x, y, z)/\partial x$, $\partial P(x, y, z)/\partial y$, and $\partial P(x, y, z)/\partial z$ can be used in practice for soft tissue elasticity mapping, despite structural and anatomical variations [3].

Vaginal Tactile Imager

The VTI, model 2S (Advanced Tactile Imaging, Inc., NJ), was used in all test procedures. The VTI probe, as shown in figure 1, is equipped with 96 pressure (tactile) sensors spaced at 2.5 mm consecutively on both sides of the probe, an orientation sensor, and temperature controllers to provide the probe temperature close to a human body before the examination. During the clinical procedure, the probe is used to acquire pressure responses from two opposite vaginal walls along the vagina. The VTI data are sampled from the probe sensors and displayed on the VTI monitor in real time. The resulting pressure maps (tactile images) of the vagina integrate all the acquired pressure and positioning data for each of the pressure sensing elements. Additionally, the VTI records the dynamic contraction for pelvic floor muscles with resolution of 1 mm. A lubricating jelly is used for patient comfort and to provide reproducible boundary/contact conditions with deformed tissues.

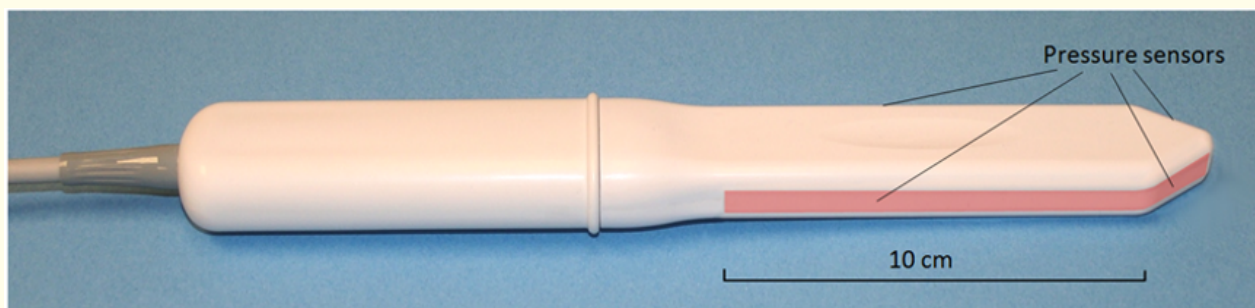


Figure 1: Vaginal tactile imaging probe. Pressure sensors are aligned on the outer surfaces of the probe (highlighted in the image).

This VTI probe allows 3 - 15 mm tissue deformation at the probe insertion (Tests 1), 20 - 45 mm tissue deformation at the probe elevation (Test 2), 5 - 7 mm deformation at the probe rotation (Test 3) and recording of dynamic responses at pelvic muscle contractions (Tests 4 - 8). The probe maneuvers in Tests 1 - 3 allow accumulation of multiple pressure patterns from the tissue surface to compose an integrated tactile image for the investigated area using a proprietary image composition algorithm similar to the imaging of the prostate and breast [11,12]. The spatial gradients $\partial P(x, y)/\partial y$ for anterior and posterior compartments are calculated within the acquired tactile images in test 1 and 2; y-coordinate is directed orthogonally from the vaginal channel, x-coordinate is located on the vaginal channel. The VTI software includes data analysis tools and reporting functions. It visualizes the anatomy, pressure maps, and calculates (automatically) 52 VTI parameters for eight test procedures. The VTI examination procedure consists of eight test-maneuvers: 1) probe insertion, 2) elevation, 3) rotation, and 4) Valsalva maneuver, 5) voluntary muscle contraction, 6) voluntary muscle contraction (left versus right side), 7) involuntary relaxation, and 8) reflex muscle contraction (cough). Tests 1 - 5 and 7 - 8 provide data for anterior/posterior compartments; test 6 provides data for left/right sides (see table 1).

Test No.	Procedure	Output
Test 1	Probe insertion	Tactile image for vaginal anterior and posterior compartments along the entire vagina (resistance, force, work, tissue elasticity)
Test 2	Probe elevation	Tactile image for anterior and posterior compartments which related to pelvic floor support structures (pressure value sand pressure gradients for specified/critical locations)
Test 3	Probe rotation	Tactile images for left and right sides along the entire vagina (force and pressure values for specified positions/locations)
Test 4	Valsalva maneuver	Dynamic pressure response from opposite sites (anterior vs posterior) along the entire vagina (changes in force and pressure; pressure peak displacements).
Test 5	Voluntary muscle contraction	Dynamic pressure response from opposite sites (anterior vs posterior) along the entire vagina (changes in force and pressure; maximum pressure values).
Test 6	Voluntary muscle contraction (sides)	Dynamic pressure response from opposite sides (left vs right) along the entire vagina (changes in force and pressure; maximum pressure values).
Test 7	Involuntary relaxation	Dynamic pressure response from opposite sites (anterior vs posterior) along the entire vagina (changes in pressure).
Test 8	Reflex muscle contraction (cough)	Dynamic pressure response from opposite sites (anterior vs posterior) along the entire vagina (changes in force and pressure; pressure peak displacements).

Table 1: VTI Examination includes 8 procedure tests.

The VTI absolute measurement accuracy is as follows: ± 0.2 kPa within 10 kPa range, ± 0.5 kPa at 25 kPa, ± 1.0 kPa at 60 kPa. The VTI relative pressure measurement accuracy lies in the range between ± 0.05 kPa to ± 0.1 kPa. The VTI pressure measurement resolution is 0.001 kPa. The VTI absolute measurement accuracy for probe orientation is ± 0.5 degree and $\pm 0.1^\circ\text{C}$ for measuring the temperature inside the probe on the surface of the pressure sensors. The VTI probe was calibrated immediately before every subject examination; it was cleaned and disinfected between the patients.

Biomechanical Mapping Parameters

Table 2 lists 52 biomechanical parameters being calculated for every participating subject based on VTI data recorded in tests 1 – 8. Anatomical assignment of the targeting/contributing pelvic structures into the specified parameters is based on the pelvic anatomy and VTI probe design [8,13-18].

No.	VTI Test	Parameters Abbreviation	Units	Parameter Description	Parameter Interpretation	Parameter Class	Targeting/Contributing Pelvic Structures
1	1	Fmax	N	Maximum value of force measured during the VTI probe insertion [9]	Maximum resistance of anterior vs posterior widening; tissue elasticity at specified location (capability to resist to applied deformation)	Maximum vaginal tissue elasticity at specified location	Tissues behind the anterior and posterior vaginal walls at 3-15 mm depth
2	1	Work	mJ	Work completed during the probe insertion (Work = Force × Displacement) [9]	Integral resistance of vaginal tissue (anterior and posterior) along the probe insertion	Average vaginal tissue elasticity	Tissues behind the anterior and posterior vaginal walls at 3-15 mm depth
3	1	Gmax_a	kPa/mm	Maximum value of anterior gradient (change of pressure per anterior wall displacement in orthogonal direction to the vaginal channel)	Maximum value of tissue elasticity in anterior compartment behind the vaginal at specified location	Maximum value of anterior tissue elasticity	Tissues/structures in anterior compartment at 10-15 mm depth
4	1	Gmax_p	kPa/mm	Maximum value of posterior gradient (change of pressure per posterior wall displacement in orthogonal direction to the vaginal channel)	Maximum value of tissue elasticity in posterior compartment behind the vaginal at specified location	Maximum value of posterior tissue elasticity	Tissues/structures in anterior compartment at 10-15 mm depth
5	1	Pmax_a	kPa	Maximum value of pressure per anterior wall along the vagina	Maximum resistance of anterior tissue to vaginal wall deformation	Anterior tissue elasticity	Tissues/structures in anterior compartment
6	1	Pmax_p	kPa	Maximum value of pressure per posterior wall along the vagina	Maximum resistance of posterior tissue to vaginal wall deformation	Posterior tissue elasticity	Tissues/structures in posterior compartment
7	2	P1max_a	kPa	Maximum pressure at the area of pubic bone	Proximity of pubic bone to vaginal wall and perineal body strength	Anatomic aspects and tissue elasticity	Tissues between vagina and pubic bone; perineal body
8	2	P2max_a	kPa	Maximum pressure at the area of urethra	Elasticity/mobility of urethra	Anatomic aspects and tissue elasticity	Urethra and surrounding tissues
9	2	P3max_a	kPa	Maximum pressure at the cervix area	Mobility of uterus and conditions of uterosacral and cardinal ligaments	Pelvic floor support	Uterosacral and cardinal ligaments

10	2	P1max_p	kPa	Maximum pressure at the perineal body	Pressure feedback of Level III support	Pelvic floor support	Puboperineal, puborectal muscles
11	2	P2max_p	kPa	Maximum pressure at middle third of vagina	Pressure feedback of Level II support	Pelvic floor support	Pubovaginal, puboanal muscles
12	2	P3max_p	kPa	Maximum pressure at upper third of vagina	Pressure feedback of Level I support	Pelvic floor support	Iliococcygeal muscle, levator plate
13	2	G1max_a	kPa/mm	Maximum gradient at the area of pubic bone	Vaginal elasticity at pubic bone area	Anterior tissue elasticity	Tissues between vagina and pubic bone; perineal body
14	2	G2max_a	kPa/mm	Maximum gradient at the area of urethra	Mobility and elasticity of urethra	Urethral tissue elasticity	Urethra and surrounding tissues
15	2	G3max_a	kPa/mm	Maximum gradient at the cervix area	Conditions of uterosacral and cardinal ligaments	Pelvic floor support	Uterosacral and cardinal ligaments
16	2	G1max_p	kPa/mm	Maximum gradient at the perineal body	Strength of Level III support (tissue deformation up to 25 mm)	Pelvic floor support	Puboperineal, puborectal muscles
17	2	G2max_p	kPa/mm	Maximum gradient at middle third of vagina	Strength of Level II support (tissue deformation up to 35 mm)	Pelvic floor support	Pubovaginal, puboanal muscles
18	2	G3max_p	kPa/mm	Maximum gradient at upper third of vagina	Strength of Level I support (tissue deformation up to 45 mm)	Pelvic floor support	Iliococcygeal muscle, levator plate
19	3	Pmax	kPa	Maximum pressure at vaginal walls deformation by 7 mm [9]	Hard tissue or tight vagina	Vaginal tissue elasticity	Tissues behind the vaginal walls at 5-7 mm depth
20	3	Fap	N	Force applied by anterior and posterior compartments to the probe [9].	Integral strength of anterior and posterior compartments	Vaginal tightening	Tissues behind anterior/posterior vaginal walls.
21	3	Fs	N	Force applied by entire left and right sides of vagina to the probe [9].	Integral strength of left and right sides of vagina	Vaginal tightening	Vaginal right/left walls and tissues behind them.
22	3	P1_l	kPa	Pressure response from a selected location (irregularity 1) at left side	Hard tissue on left vaginal wall	Irregularity on vaginal wall	Tissue/muscle behind the vaginal walls on left side.
23	3	P2_l	kPa	Pressure response from a selected location (irregularity 2) at left side	Hard tissue on left vaginal wall	Irregularity on vaginal wall	Tissue/muscle behind the vaginal walls on left side.
24	3	P3_r	kPa	Pressure response from a selected location (irregularity 3) at right side	Hard tissue on right vaginal wall	Irregularity on vaginal wall	Tissue/muscle behind the vaginal walls on right side.
25	4	dF_a	N	Integral force change in anterior compartment at Valsalva maneuver	Pelvic function* at Valsalva maneuver	Pelvic function	Multiple pelvic muscle*

26	4	dPmax_a	kPa	Maximum pressure change in anterior compartment at Valsalva maneuver.	Pelvic function* at Valsalva maneuver	Pelvic function	Multiple pelvic muscle*
27	4	dL_a	mm	Displacement of the maximum pressure peak in anterior compartment	Mobility of anterior structures*Valsalva maneuver	Pelvic function	Urethra, pubovaginal muscle; ligaments*
28	4	dF_p	N	Integral force change in posterior compartment at Valsalva maneuver	Pelvic function* at Valsalva maneuver	Pelvic function	Multiple pelvic muscle*
29	4	dPmax_p	kPa	Maximum pressure change in posterior compartment at Valsalva maneuver.	Pelvic function* at Valsalva maneuver	Pelvic function	Multiple pelvic muscle*
30	4	dL_p	mm	Displacement of the maximum pressure peak in posterior compartment	Mobility of posterior structures*Valsalva maneuver	Pelvic function	Anorectal, puborectal, pubovaginal muscles; ligaments*
31	5	dF_a	N	Integral force change in anterior compartment at voluntary muscle contraction	Integral contraction strength of pelvic muscles along the vagina	Pelvic function	Puboperineal, puborectal, pubovaginal and ilio-cygeal muscles; uretra
32	5	dPmax_a	kPa	Maximum pressure change in anterior compartment at voluntary muscle contraction	Contraction strength of specified pelvic muscles	Pelvic function	Puboperineal, puborectal and pubovaginal muscles
33	5	Pmax_a	kPa	Maximum pressure value in anterior compartment at voluntary muscle contraction.	Static and dynamic peak support of the pelvic floor	Pelvic function	Puboperineal and puborectal muscles*
34	5	dF_p	N	Integral force change in posterior compartment at voluntary muscle contraction	Integral contraction strength of pelvic muscles along the vagina	Pelvic function	Puboperineal, puborectal, pubovaginal and ilio-cygeal muscles
35	5	dPmax_p	kPa	Maximum pressure change in posterior compartment at voluntary muscle contraction	Contraction strength of pelvic muscles at specified location	Pelvic function	Puboperineal, puborectal and pubovaginal muscles

36	5	Pmax_p	kPa	Maximum pressure value in posterior compartment at voluntary muscle contraction.	Static and dynamic peak support of the pelvic floor	Pelvic function	Puboperineal and puborectal muscles*
37	6	dF_r	N	Integral force change in right side at voluntary muscle contraction	Integral contraction strength of pelvic muscles along the vagina	Pelvic function	Puboperineal, puborectal, and pubovaginal muscles
38	6	dPmax_r	kPa	Maximum pressure change in right side at voluntary muscle contraction	Contraction strength of specific pelvic muscle	Pelvic function	Puboperineal or puborectal or pubovaginal muscles
39	6	Pmax_r	kPa	Maximum pressure value in right side at voluntary muscle contraction	Specified pelvic muscle contractive capability and integrity	Pelvic function	Puboperineal or puborectal muscles
40	6	dF_l	N	Integral force change in left side at voluntary muscle contraction	Integral contraction strength of pelvic muscles along the vagina	Pelvic function	Puboperineal, puborectal, and pubovaginal muscles
41	6	dPmax_l	kPa	Maximum pressure change in left side at voluntary muscle contraction	Contraction strength of specific pelvic muscle	Pelvic function	Puboperineal or puborectal or pubovaginal muscles
42	6	Pmax_l	kPa	Maximum pressure value in left side at voluntary muscle contraction	Specified pelvic muscle contractive capability and integrity	Pelvic function	Puboperineal or puborectal muscles
43	7	dPdt_a	kPa/s	Anterior absolute pressure change per second for maximum pressure at involuntary relaxation	Innervation status of specified pelvic muscles	Innervations status	Levator ani muscles
44	7	dpcdt_a	%/s	Anterior relative pressure change per second for maximum pressure at involuntary relaxation	Innervation status of specified pelvic muscles	Innervations status	Levator ani muscles
45	7	dPdt_p	kPa/s	Posterior absolute pressure change per second for maximum pressure at involuntary relaxation	Innervation status of specified pelvic muscles	Innervations status	Levator ani muscles

46	7	dpcdt_p	%/s	Posterior relative pressure change per second for maximum pressure at involuntary relaxation	Innervation status of specified pelvic muscles	Innervations status	Levator ani muscles
47	8	dF_a	N	Integral force change in anterior compartment at reflex pelvic muscle contraction (cough)	Integral pelvic function* at reflex muscle contraction	Pelvic function	Multiple pelvic muscle*
48	8	dPmax_a	kPa	Maximum pressure change in anterior compartment at reflex pelvic muscle contraction (cough).	Contraction strength of specified pelvic muscles	Pelvic function	Multiple pelvic muscle*
49	8	dL_a	mm	Displacement of the maximum pressure peak in anterior compartment	Mobility of anterior structures*at reflex muscle contraction	Pelvic function	Urethra, pubovaginal muscle; ligaments*
50	8	dF_p	N	Integral force change in posterior compartment at reflex pelvic muscle contraction (cough)	Integral pelvic function* at reflex muscle contraction	Pelvic function	Multiple pelvic muscle*
51	8	dPmax_p	kPa	Maximum pressure change in posterior compartment at reflex pelvic muscle contraction (cough).	Contraction strength of specified pelvic muscles	Pelvic function	Multiple pelvic muscle*
52	8	dL_p	mm	Displacement of the maximum pressure peak in posterior compartment	Mobility of anterior structures*at reflex muscle contraction	Pelvic function	Anorectal, puborectal and pubovaginal muscles; ligaments*

Table 2: VTI biomechanical parameters.

Population Description

Sixty subjects with normal and UP conditions were included in the data analysis from multi-site observational, case-controlled studies (clinical trials identifiers NCT02294383 and NCT0292558). Each subject’s age, height, weight, and parity distribution data are present in table 3. Prior to the VTI examination, a standard physical examination was performed, including a bimanual pelvic examination and Pelvic Organ Prolapse Quantification (POP-Q) [19]. Employing this approach, we found that 42 subjects had normal pelvic floor conditions (no POP, no SUI) and 18 had predominate uterine prolapse conditions (no significant anterior or posterior prolapse). Among subjects with UP conditions, we found 11 had uterine Stage III prolapse, 6 had uterine Stage II prolapse and one had Stage I uterine prolapse, 8 suffered from SUI, 2 had urinary urgency, and one had fecal incontinence. None of the analyzed subjects had a prior history of pelvic floor surgery. The clinical protocol was approved by the Institutional Review Board and all women provided written informed consent to be enrolled into the study. This clinical research was done in compliance with the Health Insurance Portability and Accountability Act. The VTI examination data for eight Tests (see Table 1) were obtained and recorded at the time of the scheduled routine urogynecologic visits.

Citation: Vladimir Egorov, et al. “Biomechanical Mapping of the Female Pelvic Floor: Uterine Prolapse Versus Normal Conditions”. *EC Gynaecology* 7.11 (2018): 431-446.

Total study workflow comprised of the following steps: (1) Recruiting women who routinely undergo vaginal examination as a part of their diagnostic treatment of concerned areas; (2) Acquisition of clinical diagnostic information related to the studied cases by standard clinical means; (3) Performing a VTI examination in lithotomic position; (4) Analyzing VTI data and assessment of the VTI parameters for pelvic floor characterization for normal versus UP conditions.

Statistical Analysis

52 biomechanical parameters were calculated automatically per each of the 60 analyzed VTI examinations or cases (one VTI examination per each subjects). In some rare cases the parameter calculation required a manual correction of the anatomical location where the parameters must be calculated. Unpaired t-test (normal versus UP group) was completed per parameter to determine whether the parameter showed dependence on the pelvic floor conditions. For visual evaluation of the analyzed clinical data distributions we used notched boxplots [20] showing a confidence interval for the median value (central horizontal line), 25% and 75% quartiles. The spacing between the different parts of the box helps to compare variance. The boxplot also determines skewness (asymmetry) and outlier (cross). The intersection or divergence of confidence intervals for two patient samples is a visual analog of the t-test. The MATLAB (MathWorks, MA) statistical functions were used for the data analysis.

Results

Table 3 displays the calculated statistics (hypothesis testing outcome H- and p-value) for UP versus normal (Norm) conditions, average (Aver) values for 52 biomechanical parameters, standard deviations (SD), and the ranges (Min, Max) for both UP group (18 subjects) and normal group (42 subjects).

		<i>H</i>	<i>p</i>	Units	Aver Norm	Aver UP	SD Norm	SD UP	Min Norm	Min UP	Max Norm	Max UP
Height →	0	0.5106	cm	161.7	163.6	11.9	5.5	125	152	180	174	
Weight →	0	0.3790	kg	151.2	158.1	26.5	29.9	110	115	200	224	
Age →	0	0.3763	y.o.	51.2	54.8	16.0	10.5	26	37	90	75	
Parity (P) →	1	0.0003	-	1.4	2.7	1.0	1.5	0	1	3	6	
Parameters number ↓	Test↓											
1	1	1	0.0493	N	1.24	0.86	0.74	0.51	0.23	0.30	4.05	2.04
2	1	0	0.4490	mJ	42.34	37.60	22.46	21.12	4.50	14.90	96.30	93.20
3	1	0	0.1543	kPa/mm	2.38	1.55	2.21	1.52	0.21	0.13	11.48	5.26
4	1	0	0.0624	kPa/mm	1.57	0.99	1.08	1.07	0.17	0.13	5.06	4.02
5	1	1	0.0081	kPa	39.43	20.67	26.78	16.75	6.00	3.90	145.50	65.30
6	1	1	0.0243	kPa	22.64	13.83	14.33	11.31	5.10	3.70	60.90	46.70
7	2	0	0.0826	kPa	28.24	20.42	15.13	17.03	4.50	2.90	70.50	63.60
8	2	1	0.0054	kPa	11.85	6.28	7.72	4.00	0.10	2.10	31.80	15.40
9	2	0	0.2315	kPa	8.51	6.13	8.03	3.22	0.00	3.00	40.70	13.60
10	2	1	0.0107	kPa	13.80	7.41	9.65	5.27	2.10	2.70	53.60	18.80
11	2	1	0.0475	kPa	9.54	6.26	6.41	3.64	1.60	2.00	29.20	15.10
12	2	0	0.8892	kPa	6.94	7.22	7.62	5.24	0.40	2.10	44.00	24.00
13	2	0	0.1135	kPa/mm	1.89	1.21	1.66	1.01	0.00	0.06	6.15	3.40
14	2	1	0.0163	kPa/mm	0.79	0.29	0.84	0.24	0.00	0.08	3.95	1.10
15	2	0	0.1297	kPa/mm	0.57	0.31	0.67	0.45	0.00	0.08	3.30	2.07

16	2	0	0.1024	kPa/mm	0.73	0.36	0.90	0.38	0.06	0.03	4.91	1.13
17	2	1	0.0213	kPa/mm	0.41	0.24	0.30	0.18	0.05	0.05	1.16	0.68
18	2	0	0.7162	kPa/mm	0.44	0.38	0.60	0.41	0.00	0.05	3.48	1.80
19	3	1	0.0009	kPa	32.16	17.19	15.51	14.16	5.04	4.79	69.40	50.30
20	3	1	0.0415	N	4.03	2.97	1.91	1.57	1.26	1.05	9.15	6.93
21	3	0	0.0719	N	1.19	1.64	0.83	1.01	0.10	0.17	3.49	3.88
22	3	0	0.0962	kPa	9.21	6.28	6.36	5.59	2.30	1.40	30.70	22.10
23	3	0	0.2368	kPa	4.93	3.93	3.14	2.58	0.80	0.90	12.90	10.10
24	3	1	0.0102	kPa	9.86	5.48	6.43	4.13	2.40	1.30	25.50	16.50
25	4	1	0.0273	N	1.24	1.78	0.80	0.84	0.31	0.38	3.78	3.22
26	4	0	0.1791	kPa	10.63	6.56	10.81	9.03	-4.30	-12.80	40.20	33.20
27	4	1	0.0062	mm	1.83	7.18	5.02	8.53	-12.30	-4.00	13.50	27.80
28	4	1	0.0197	N	1.22	1.84	0.89	0.88	0.05	0.29	4.07	3.33
29	4	0	0.6940	kPa	6.80	7.45	6.06	4.61	0.20	1.20	21.60	18.20
30	4	0	0.1454	mm	2.39	4.90	5.52	6.40	-10.00	-0.30	18.80	22.80
31	5	0	0.1937	N	1.57	1.22	0.99	0.88	0.30	0.31	5.89	3.12
32	5	0	0.1796	kPa	22.27	16.12	15.44	17.46	1.80	1.80	80.40	56.50
33	5	1	0.0118	kPa	40.86	26.54	19.26	20.19	4.40	6.70	99.40	69.70
34	5	0	0.0975	N	1.84	1.28	1.27	0.92	0.31	0.26	5.87	3.53
35	5	1	0.0084	kPa	13.86	7.28	9.62	5.17	2.00	1.50	44.40	19.80
36	5	1	0.0003	kPa	22.75	12.52	10.75	5.40	5.60	3.50	49.00	21.70
37	6	0	0.8509	N	0.85	0.89	0.64	0.72	0.09	0.08	2.77	2.62
38	6	0	0.0964	kPa	7.68	4.96	6.11	4.31	0.20	0.40	23.60	15.60
39	6	1	0.0218	kPa	13.32	8.16	8.35	5.70	2.20	1.20	29.50	22.70
40	6	0	0.8424	N	0.85	0.89	0.71	0.79	0.09	0.09	3.18	3.07
41	6	0	0.1046	kPa	6.92	4.53	5.54	3.76	0.50	0.20	20.60	14.50
42	6	1	0.0329	kPa	12.37	7.78	8.28	4.51	2.60	1.90	28.40	16.30
43	7	0	0.7871	kPa/s	-1.29	-1.42	1.63	1.62	-6.44	-6.34	0.72	0.01
44	7	1	0.0102	%/s	-3.10	-5.95	3.56	4.05	-11.70	-12.70	4.30	0.10
45	7	0	0.4867	kPa/s	-1.01	-0.78	1.35	0.67	-6.10	-3.02	0.37	0.02
46	7	1	0.0415	%/s	-4.11	-6.57	3.84	4.61	-13.00	-15.90	1.40	1.10
47	8	0	0.5853	N	2.26	2.05	1.42	0.97	0.13	0.89	5.53	3.98
48	8	0	0.1895	kPa	13.93	8.79	14.94	8.85	-17.30	-6.50	61.50	31.40
49	8	0	0.0985	mm	6.52	10.09	4.71	10.28	-3.50	-4.80	17.30	27.50
50	8	0	0.8881	N	2.25	2.19	1.50	1.18	0.43	0.88	5.19	4.96
51	8	0	0.1376	kPa	11.41	8.27	8.22	4.19	1.00	2.50	27.30	17.30
52	8	0	0.9416	mm	3.65	3.51j	6.33	6.92	-5.00	-10.00	20.00	17.00

Table 3: Biomechanical Parameters: Uterine prolapse (group of 18 subjects) versus normal conditions (group of 42 subjects).

The t-tests for the UP group of 18 subjects versus a normal group of 42 subjects demonstrate that 22 out of 52 parameters have statistically significant differences between the groups and these parameters have the potential to be used for detection and description of UP conditions. The analyzed groups have the same subject height and weight distributions. At the same time, these primary analyzed groups have differences in parity with averages P = 1.4 and 2.7 per the group (see table 2).

Further, figures 2-7 show the discovered with the VTI changes in the female pelvic floor with the UP. Figure 2 displays two cases with normal pelvic support (no POP) and with uterine Stage II prolapse; its comparison demonstrates significant difference in tissue elasticity along the anterior and posterior compartments.

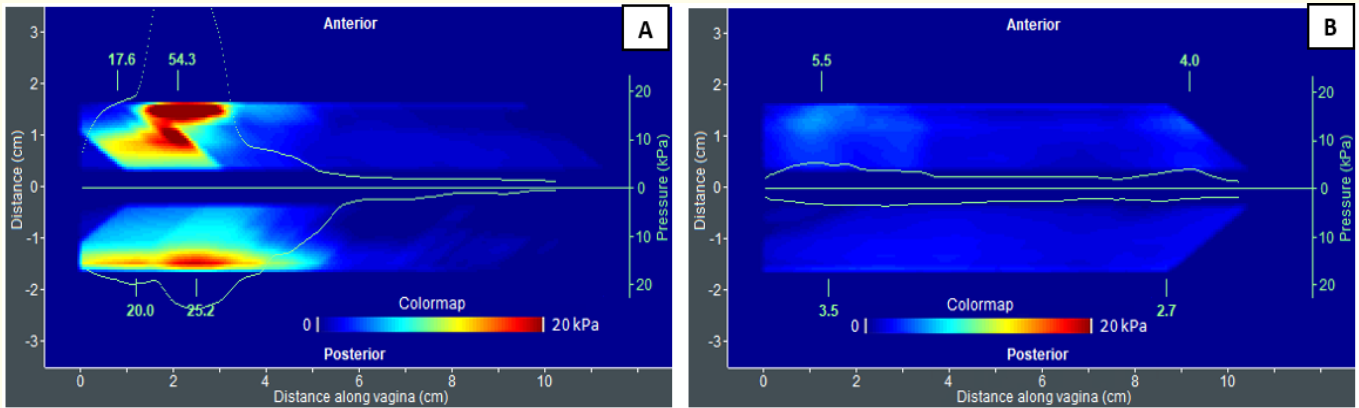


Figure 2: VTI Test 1 results for (A) 57 y.o. patient with normal pelvic conditions and (B) 44 y.o. patient with uterine Stage II prolapse.

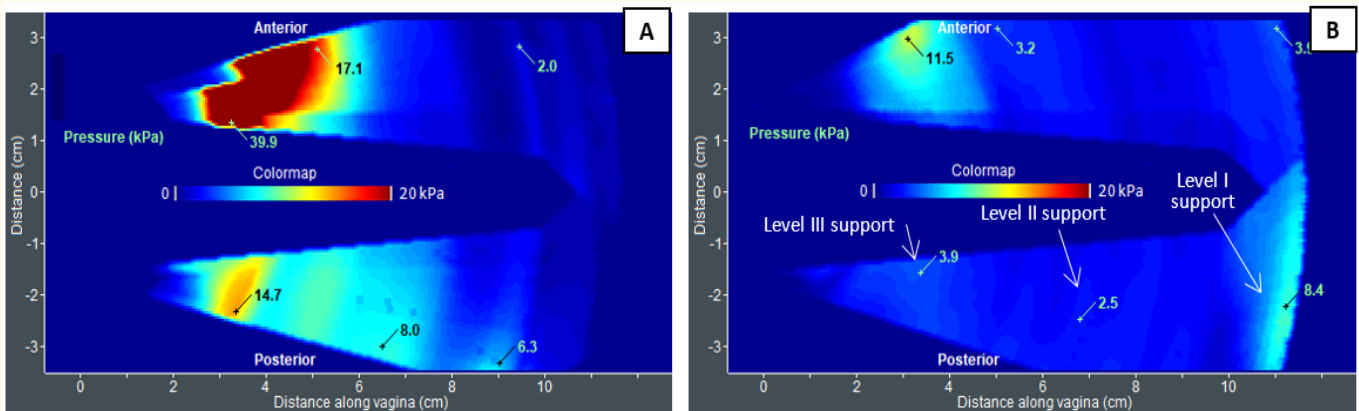


Figure 3: VTI Test 2 results for (A) 51 y.o. patient with normal pelvic conditions and (B) 61 y.o. patient with uterine Stage III prolapse.

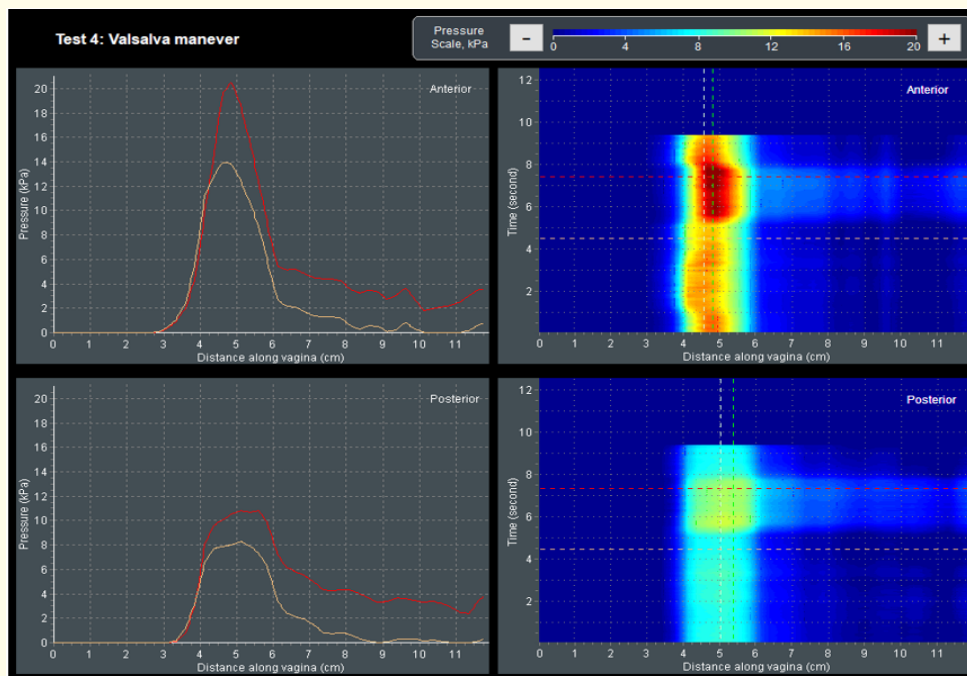


Figure 4: VTI Test 4 results for 42 y.o. patient with normal pelvic support.

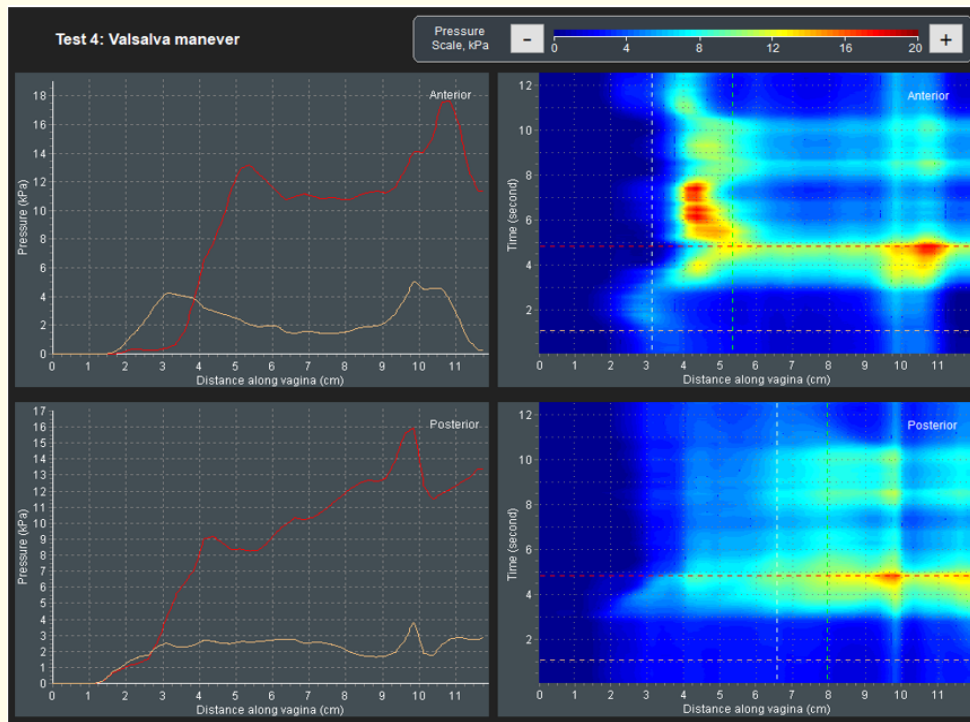


Figure 5: VTI Test 4 results for 54 y.o. patient with uterine Stage III prolapse.

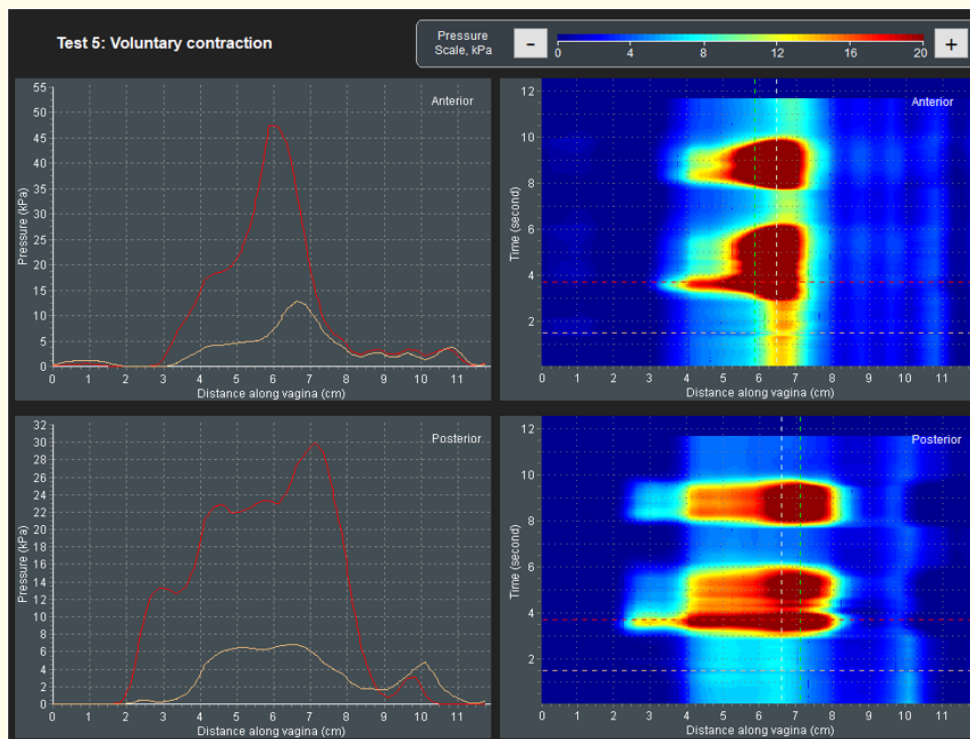


Figure 6: VTI Test 5 results for 68 y.o. patient with normal pelvic support conditions.

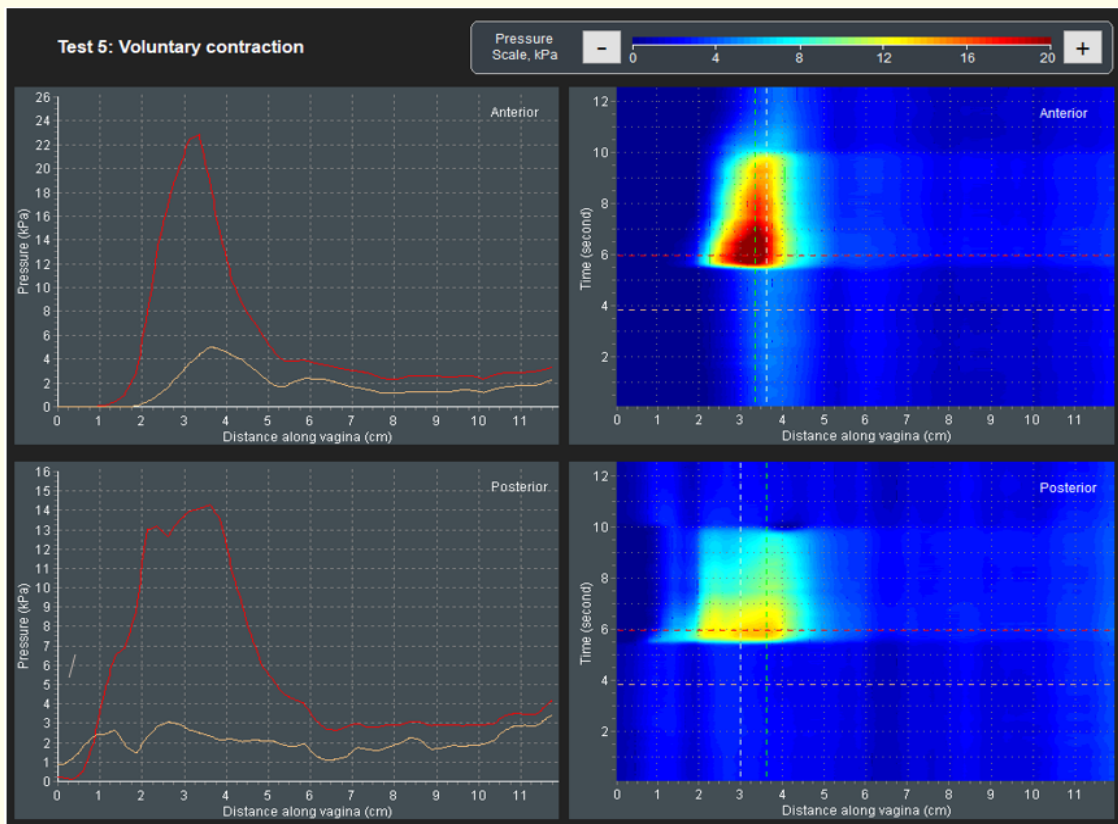


Figure 7: VTI Test 5 results for 66 y.o. patient with uterine Stage III prolapse.

Figure 8 displays the boxplots for selected parameters for UP versus normal groups presented in table 2.

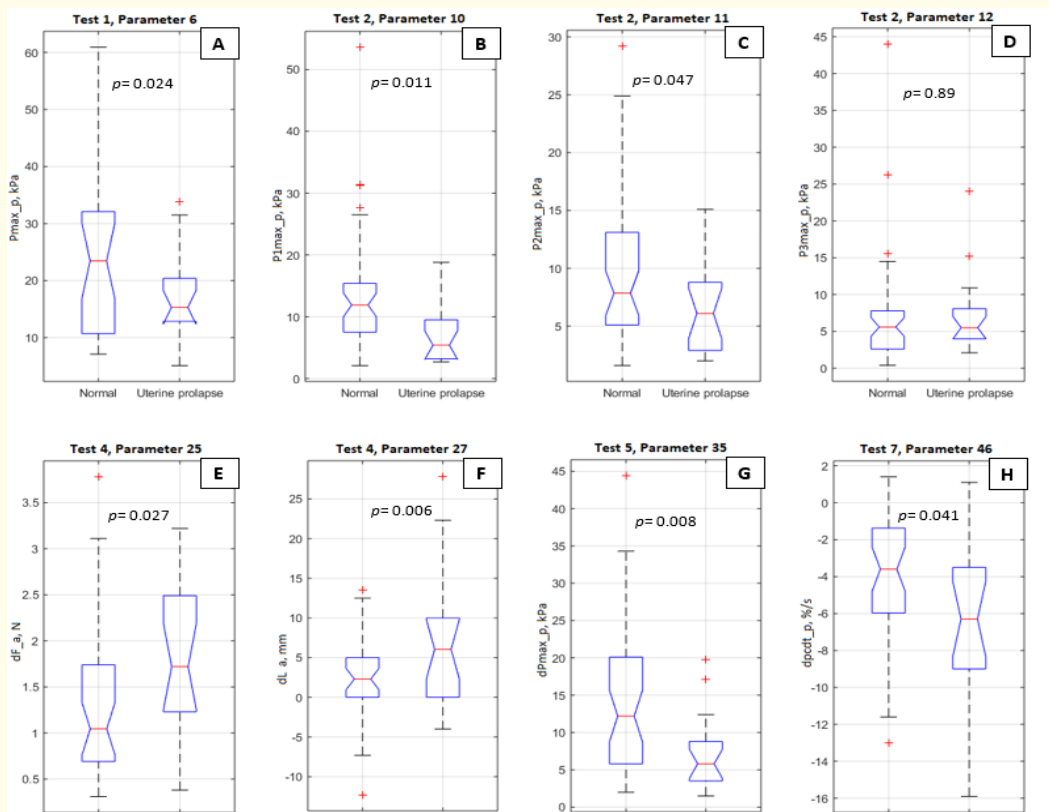


Figure 8: Displays the boxplots for selected parameters for UP versus normal groups presented in table 2.

Discussion

The results of this research are in agreement with previously reported data [3-10]. However, this study includes the analysis of only urine prolapse (UP) versus normal conditions (no POP) and the largest comprehensive VTI parameter set ever considered. Twenty-two of 52 biomechanical parameters were identified to possess statistically significant sensitivity to UP versus normal pelvic conditions (see Table 2). The average changes of these parameters were recorded to be from 36.0% to 293% (83.4% in average). These changes with UP clearly outperform possible deviations related to VTI intra- and inter-operator variability, which were found on an average of $\pm 15.1\%$ (intra-observer error) and ± 18.4 (inter-observer error) [7]. These reproducibility errors have value and sign intrinsically by a chance, but the study identified statistically systematical parameter changes with the UP.

Test 1 provides three identified parameters (1, 5, 6) related to tissue elasticity; their average values change from 44.9% to 90.8% for normal relative to UP conditions. Test 2 provides 5 identified parameters (8, 10, 11, 14, 17) related to the pelvic support structure; their average values escalate from 75.5% to 173.6% for normal relative to UP conditions. Test 3 provides 3 identified parameters (19, 20, 24) related to tissue elasticity; their average values increase from 36.0% to 87.1% for normal relative to UP conditions. Test 4 provides 3 identified parameters (25, 27, 28) related to pelvic function, the values of which change from 43.4% to 293.3% for UP relative to normal conditions. Test 5 provides 3 identified parameters (33, 35, 36) related to pelvic function; their average values change from 53.9% to 90.3% for normal relative to UP conditions. Test 6 provides 2 identified parameters (39, 42) related to pelvic function; their average values change from 58.9% to 63.3% for normal relative to UP conditions. Test 7 provides 2 identified parameters (44, 46) related to pelvic function; their average values change from 60.0% to 91.8% for UP relative to normal conditions. Test 8 provides no identified parameter sensitive to UP. In total, among the 21 identified diagnostic parameters sensitive to the pelvic conditions at UP, 5 parameters are related to tissue elasticity, 6 parameters are related to pelvic support structures, and 10 parameters are related to pelvic functions.

As seen in table 2, the analyzed groups of subjects manifest differences in parity. This seems inevitable, as the parity tends to correlate with the prevalence of the UP [21]. Further, it is important to note that the group with normal pelvic conditions (no POP, no SUI) was composed of the visitors of urogynecological site - these patients may have some pelvic floor conditions that were not identified in this study. It is possible that the patients from the normal group have had pre-prolapse conditions which haven't yet transformed into anatomically visible POP. This study reasonably proposes that if the normal group is composed of 20 - 40 y.o. subjects with no history of consulting urogynecological clinics, more significant differences for the VTI parameters versus the UP group may be observed.

The figures 2-7 for notable cases with normal and UP conditions demonstrate the differences detected in the specified VTI Tests such as (1) tissue elasticity decrease with the UP (see figure 2), (2) deterioration of Level III and Level II supports with some increase in Level I support under UP conditions (see figure 3), (3, 4) increase in anterior cumulative force and extended mobility of urethra at Valsalva maneuver with the UP (see figures 4 and 5), (5) significant decrease in pelvic muscle contractile capabilities with UP (see figure 6 and 7).

The boxplots for selected parameter distributions in figure 8 display (1) tissue elasticity decrease with the UP (see panel A), (2) deterioration of Level III and Level II supports (see panels B and C) with no change in Level I support under UP conditions (see panel D), (3, 4) increase in anterior cumulative force, and extended mobility of urethra at Valsalva maneuver with the UP (see panel E and F), (5) significant decrease in pelvic muscle contractive capabilities with UP (see panel G), and (6) faster involuntary pelvic muscle relaxation with the UP which relates with muscle innervations (see panel H).

The next step (which falls beyond the purview of this article) with these biomechanical parameters may include (a) investigation into anterior and posterior prolapse, (b) analysis for continence versus incontinence conditions, (c) analysis of urogynecological surgical outcomes as a whole as well as per specific surgical procedure, (d) combining the VTI data with urodynamics, ultrasound, and MRI data, (e) to use the VTI and other clinically related data for predicative modeling of outcomes for conservative and surgical procedures (personalized predictive treatment), and (f) maintaining the objective history of biomechanical transformation of the patient's pelvic floor with age.

One of the strengths of this study is that the current VTI offers an opportunity to assess the tissue elasticity, pelvic support structures, and pelvic function (muscle and ligaments) in high definition along the entire length of the anterior, posterior, and lateral walls at rest, with applied deflection pressures and pelvic muscle contractions. All 52 parameters are calculated automatically in real time. This allows a large body of measurements to evaluate individual variations in support defects as well as to identify specific problematic structures. In addition, the technology provides the opportunity to measure pelvic floor muscle strength at specific locations along the vaginal wall and helps correlate the relative contributions to measured tissue properties. These measurements may provide insight into the functional contribution or relationships between support tissues and the underlying muscle support for a patient. Due to the relative easy availability and cost-effectiveness of VTI testing, post-treatment follow-up is available to evaluate the surgical impact on functional tissue properties and pelvic floor muscles. This may provide valuable outcome measurements for evaluating current and future treatments for pelvic organ prolapse.

One of the shortcomings of this study was the relatively small sample size that was used. Further studies with larger patient population investigating a variety of other pelvic floor conditions and their application in the evaluation of interventions, including physical therapy, conservative management options, and surgical correction, are needed at this point to further explore the diagnostic values of the biomechanical mapping of the female pelvic floor.

Conclusions

The biomechanical mapping of the female pelvic floor with the VTI provides a unique set of quantitative parameters characterizing uterine prolapse versus normal conditions. These objectively measurable biomechanical transformations of pelvic tissues including supportive structures, and their biophysical functions under the prolapse conditions may be used in future research and practical applications.

Acknowledgements

Research reported in this publication was supported by the National Institute on Aging of the National Institutes of Health under Awards Number R44AG034714 and SB1AG034714. The content is solely the responsibility of the authors and does not necessarily represent the official views of the National Institutes of Health.

Disclosure

V. Egorov: CEO and shareholder of Advanced Tactile Imaging, Inc.

H. van Raalte: shareholder of Advanced Tactile Imaging, Inc.

Bibliography

1. Siddiqui NY, et al. "American Urogynecologic Society Prolapse Consensus Conference Summary Report". *Female Pelvic Medicine and Reconstructive Surgery* 24.4 (2018): 260-263.
2. Jeffery S and Roovers JP. "Quo vadis, vaginal mesh in pelvic organ prolapse?" *International Urogynecology Journal* 29 (2018): 1073-1074.
3. Egorov V, et al. "Vaginal Tactile Imaging". *IEEE Transactions on Biomedical Engineering* 57.7 (2010): 1736-1744.
4. Egorov V, et al. "Quantifying vaginal tissue elasticity under normal and prolapse conditions by tactile imaging". *International Urogynecology Journal* 23.4 (2012): 459-466.
5. Egorov V, et al. "Biomechanical characterization of the pelvic floor using tactile imaging". In: *Biomechanics of the Female Pelvic Floor*, Eds. Hoyte L, Damaser MS, 1st Edition, Elsevier (2016): 317-348.
6. Kim K., et al. "Emerging imaging technologies and techniques". In: *Practical Pelvic Floor Ultrasonography*, Ed. Abbas Shobeiri, 2nd Edition, Springer International Publishing AG (2017): 327-336.

7. van Raalte H., *et al.* "Intra- and inter-observer reproducibility of vaginal tactile imaging". *Female Pelvic Medicine and Reconstructive Surgery* 22.5 (2016): S130-S131.
8. Lucente V., *et al.* "Biomechanical paradigm and interpretation of female pelvic floor conditions before a treatment". *International Journal of Women's Health* 9 (2017): 521-550.
9. Egorov V., *et al.* "Quantitative Assessment and Interpretation of Vaginal Conditions". *Sexual Medicine* 6.1 (2018): 39-48.
10. van Raalte H and Egorov V. "Tactile imaging markers to characterize female pelvic floor conditions". *Open Journal of Obstetrics and Gynecology* 5.9 (2015): 505-515.
11. Egorov V., *et al.* "Prostate Mechanical Imaging: 3-D Image Composition and Feature Calculations". *IEEE Transactions on Medical Imaging* 25.10 (2006): 1329-1340.
12. Egorov V and Sarvazyan AP. "Mechanical imaging of the breast". *IEEE Transactions on Medical Imaging* 27.9 (2008): 1275-1287.
13. Egorov V., *et al.* "Biomechanical mapping of the female pelvic floor: prolapse versus normal conditions". *Open Journal of Obstetrics and Gynecology* 8.10 (2018): 900-925.
14. Shobeiri SA. "Practical Pelvic Floor Ultrasonography". A Multicompartmental Approach to 2D/3D/4D Ultrasonography of the Pelvic Floor, 2nd Edition. Springer International Publishing AG (2017): 1-368.
15. DeLancey JO. "Pelvic floor anatomy and pathology". In: Hoyte L, Damaser MS, editors. *Biomechanics of the Female Pelvic Floor*. 1st edition. London, UK: Elsevier (2016): 13-51.
16. Dietz HP. "Pelvic Floor Ultrasound. Atlas and Text Book". Creative Commons Attribution License. Springwood, Australia (2016): 1-127.
17. Hoyte L., *et al.* "Segmentations of MRI images of the female pelvic floor: a study of inter- and intra-reader reliability". *Journal of Magnetic Resonance Imaging* 33.3 (2011): 684-691.
18. Petros P. "The Female Pelvic Floor: Function, Dysfunction and Management According to the Integral Theory". 3rd edition. Berlin, Germany: Springer (2010): 1-330.
19. Bump RC., *et al.* "The standardization of terminology of female pelvic organ prolapse and pelvic floor dysfunction". *American Journal of Obstetrics and Gynecology* 175.1 (1996): 10-17.
20. McGill R., *et al.* "Variations of Box Plots". *American Statistician* 32.1 (1978): 12-16.
21. Lieschen H., *et al.* "Vaginal Parity and Pelvic Organ Prolapse". *Journal of Reproductive Medicine* 55.3-4 (2010): 93-98.

Volume 7 Issue 11 November 2018

© All rights reserved by Vladimir Egorov., *et al.*